RSC Advances

PAPER

View Article Online
View Journal | View Issue

Cite this: *RSC Adv.*, 2020, **10**, 27408

CNT modified layered α-MnO_2 hybrid flame retardants: preparation and their performance in the flame retardancy of epoxy resins

Xiaodong Qian, Congling Shi* and Jingyun Jing

In this paper, CNT modified layered α-MnO_2 hybrid flame retardants (α-MnO_2–CNTs) were synthesized through one-pot preparation. The structure and composition of the α-MnO_2–CNTs hybrid flame retardants were investigated by X-ray diffraction, TEM and SEM. Subsequently, the α-MnO_2–CNTs hybrids were then incorporated into epoxy resin (EP) to improve the fire safety properties. Compared with pure EP and the composites with CNTs or α-MnO_2, EP/α-MnO_2–CNTs composites exhibited improved flame retardancy and smoke suppression properties. With the incorporation of only 2.0 wt% of α-MnO_2–CNTs hybrid flame retardants, the peak heat release rate and total heat release of the composites showed 34% and 10.7% reduction respectively. In addition, the volatile gases such as CO and CO_2 were reduced and the smoke generation was also effectively inhibited. The improved fire safety of the composites is generally due to the network structures and the synergistic effect of α-MnO_2 and CNTs, the catalyzing charring effect, smoke suppression and the physical barrier effect of α-MnO_2 nanosheets.

Received 23rd April 2020
Accepted 8th July 2020

DOI: 10.1039/d0ra03654d

rsc.li/rsc-advances

1. Introduction

Incorporating nano-fillers into polymers is an effective method to improve the fire safety of polymer materials. Due to the incorporation of inorganic nano-fillers, the properties of the composites such as thermal stability, flame retardant properties, smoke suppression performance and mechanical properties are improved significantly.[1–3] The nano-fillers such as carbon nanotubes (CNTs), nanoclays and graphene have been widely investigated due to their superior mechanical strength, conductivity, mechanical and thermal properties.[4–6] Among various nano-fillers, CNTs are the ideal nano-fillers for improving the properties of the polymer nanocomposites. The structures, topology and dimensions of CNTs can impact the nanocomposites with great improvement of the mechanical properties, thermal stability, electrical conductivities and fire safety.[7]

The incorporation of CNTs into the polymer materials usually improves the flame retardant performance of the composites. The main reason for the improved flame retardant performance of the composites is attributed to the improved thermal stability of composites by their good heat resistance. Moreover, Kashiwagi's research found that CNTs can form a jammed network structure in the polymer matrix and give the nanocomposites with improved flame retardant properties.[8] Moreover, the dispersion of CNTs in the composites affects the fire safety and mechanical properties of the composites, but the strong van der Waals force among the CNTs usually results in the agglomeration of CNTs in the polymer matrix, which limits the properties improvement of the composites.[9,10] Generally, the dispersion of CNTs in the composites influence the properties of the composites greatly, the surface modification of CNTs plays an important roles in the production of polymer composites.

As for the modification, the acid such as HNO_3/H_2O_2 and HNO_3/H_2SO_4 are usually adopted to treat CNTs, and the CNTs will get functionalized group such as –COOH or –OH. The covalent bonding of CNTs can be achieved by the reaction between the organic group and –COOH or –OH on the surface of CNTs.[11,12] Another class of flame retardant nano-additives are 2D nano-additives, taking molybdenum sulfide, graphene and MMT for example. Among various 2D nano-additives, the structure of α-MnO_2 nanosheet has attracted great attention due to its high specific area, ultrathin thickness, strength and resilience.[13,14] Manganese is a typical transition metal element. It is found that manganese compound is a good catalyst such as the application in organic catalysis, and it is also reported that manganese compound has good catalytic charging effect. As a typical transition metallic oxide, α-MnO_2 nanosheet also has the effect of restraining the smoke, which is an good nanofillers in the flame retardancy of polymer materials.[15,16] However, similar to the CNTs, the dispersion of α-MnO_2 nanosheets in the composites is the key point of the flame retardant efficiency.

Beijing Key Laboratory of Metro Fire and Passenger Transportation Safety, China Academy of Safety Science and Technology, Beijing 100012, China. E-mail: wjxyqxd@hotmail.com; shicl@chinasafety.ac.cn; bdqyjjy@163.com

The composites based on the nano-fillers polymer which contains two or three nano-fillers has attracted great attention due to their synergistic flame retardant effects. The network structures of CNTs impart the polymer materials with excellent mechanical, electrical, thermal properties and fire-resistant properties, but the CNTs usually agglomerate in polymer matrix. α-MnO_2 nanosheet is a good catalyst and has catalytic charring and smoke suppression effects due to its layered structure. It's reported that the layers materials/CNTs hybrids have good flame retardant efficiency due to their synergistic dispersion effects.[17,18] Therefore, the α-MnO_2 nanosheet formed after CNTs hybrids run through to α-MnO_2 nanosheet can improve the dispersion of CNTs and α-MnO_2 nanosheet in the polymer matrix. Moreover, the compact network structure can also play the good synergistic role in improving the fire safety properties of the composites.

In this manuscript, CNTs modified layered α-MnO_2 hybrids flame retardants (α-MnO_2–CNTs) were prepared through one-pot preparation. The hybrids flame retardants were then introduced into EP matrix and the thermal stability, flame retardant and smoke suppression properties of the composites were investigated. The α-MnO_2–CNTs hybrids flame retardants exhibit a great improvement on improving the fire safety of epoxy resins.

2. Experimental

2.1 Raw materials

Epoxy resins (E-44, epoxy value is 0.44 mol/100 g, bisphenol A epoxy resins) were purchased from Hefei Jiangfeng Chemical Industry Co. Ltd. Potassium permanganate ($KMnO_4$), H_2O_2 (30 wt%), manganese sulfate ($MnSO_4 \cdot H_2O$) were supplied by Sinopharm Chemical Reagent Co. Ltd. (Shanghai, China). 4,4-Diamino-diphenyl methane (DDM) was supplied by Sinopharm Chemical Reagent Co. Ltd. (Shanghai, China). Moreover, carbon nanotubes (CNTs) was supplied by Chengdu Organic Chemicals Co. Ltd.

2.2 Preparation of α-MnO_2 (Mn) and α-MnO_2–CNTs hybrids flame retardants (Mn–CNTs)

The α-MnO_2 nanosheets (Mn) were prepared according to the previous work.[19] In typical procedure, 24 mL of 1.0 M tetramethylammonium hydroxide, 4 mL of 30 wt% H_2O_2 and 30 mL of deionized water were mixed and then the mixtures were poured into 40 mL of 0.3 M $MnCl_2$ aqueous within 15 seconds. The dark brown mixtures were stirred overnight at ambient temperature. Then, the mixtures were filtered and washed with deionized water for three times, and the products were dried at room temperature for further use. Then the α-MnO_2 nanosheets named Mn were obtained.

The preparation processes of α-MnO_2–CNTs hybrids flame retardants (Mn–CNTs) were prepared as follows: 24 mL of 1.0 M tetramethylammonium hydroxide, 4 mL of 30 wt% H_2O_2, 30 mL of deionized and 0.2 g of CNTs were mixed and then the mixtures were poured into 40 mL of 0.3 M $MnCl_2$ aqueous within 15 seconds. The black mixtures were stirred overnight at ambient temperature. Then, the mixtures were filtered and washed with deionized water for three times, and the products were dried at room temperature for further use. The product named Mn–CNTs was obtained. The preparation process of α-MnO_2–CNTs hybrids flame retardants are shown in Scheme 1.

2.3 Preparation of the composites

The preparation of epoxy composites with only 2 wt% Mn–CNTs content was as follows: epoxy resins (100 g) and Mn–CNTs (2.4 g) were mixed and the mixtures were added into a 250 mL three-necked flask equipped with a magnetic stirrer. The temperature of the mixture was increased to 100 °C and kept stirring for 3 hours, and DDM (21.7 g, meltdown) was added into the mixtures. The mixtures were then cured at 100 °C for 2 hours and then 150 °C for 2 hours. After that, the samples were cooled to room temperature and the EP/Mn–CNTs composite was obtained. Pristine EP/CNTs and EP/Mn composites at the flame retardants loading of 2 wt% were also prepared under the same processing conditions. The composition of resins is presented in Table 1 and

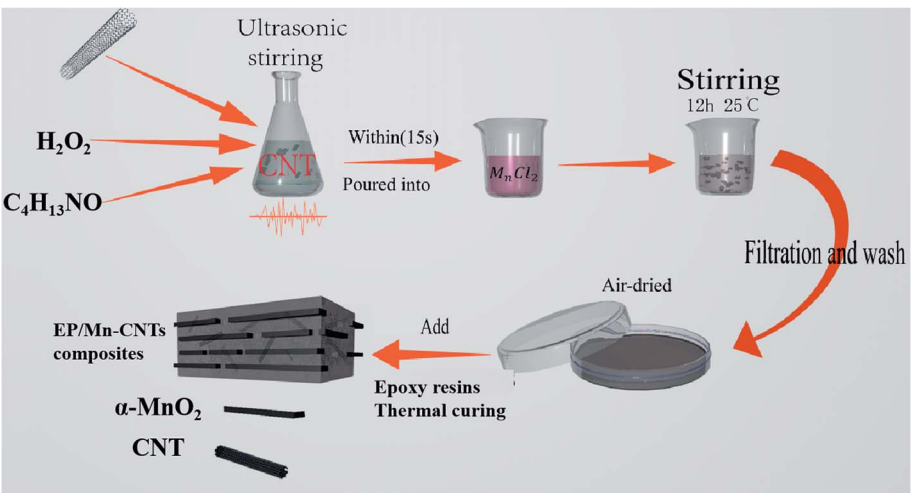

Scheme 1 The preparation process of α-MnO_2–CNTs hybrids and its polymer composites.

the synthesis of EP/Mn–CNTs composites is illustrated in Scheme 1.

2.4 Characterization

The wavelength range of the FTIR spectroscopy was 4000–500 cm^{-1}. The instrument was recorded with Nicolet 6700 FT-IR spectrophotometer and the thin KBr slice was used.

The structures of CNTs as well as the nanocomposites were investigated by transmission electron microscopy (TEM) (JEOL JEM-2100 instrument).

TGA Q5000 IR thermal gravimetric analyzer (TA Instruments) was adopted to investigate the thermal stability of the composites. Through the thermogravimetric analysis (TGA) test, about 4–10 mg of samples was heated from room temperature to 800 °C.

The flammability of the samples was investigated by cone calorimeter according to ISO 5660 and the heat flux is 50 kW m^{-1}. The dimensions of the samples are 100 × 100 × 3 mm^3. Each sample is tested for three times and the average one is adopted in the manuscript. The surface structures of the composites and the char layers are investigated by scanning electron microscope (SEM). The samples were coated with gold layer.

Raman spectroscopy measurements of the char layers were investigated by SPEX-1403 laser Raman spectrometer (SPEX Co., USA) at room temperature.

Table 1 The corresponding data of TGA for pure EP and its composites in nitrogen atmosphere

Samples	FRs contents	$T_{-10\%}$/°C	T_{max}/°C	Char residues at 700 °C/%
EP	0	386	399	13.9
EP/CNTs	CNTs: 2%	382	397	16.5
EP/Mn	α-MnO_2: 2%	355	373	17.5
EP/Mn–CNTs	α-MnO_2–CNTs: 2%	359	363	18.9

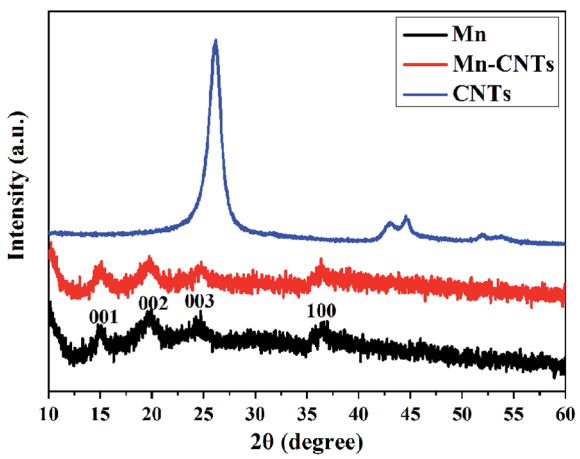

Fig. 1 The XRD result of CNTs, α-MnO_2 and α-MnO_2–CNTs.

3. Results and discussion

3.1 Characterization of α-MnO_2 and α-MnO_2–CNTs hybrids

Fig. 1 shows X-ray diffraction pattern of α-MnO_2, α-MnO_2–CNTs hybrids and CNTs. As for peaks of CNTs at 25.44° (002) and 42.5° (100), they are attributed to the hexagonal graphite structure. The characteristic peaks of α-MnO_2 nanosheet at 15.51° (001), 19.83° (002), 2.68° (003) and 36.54° (100) (reference to JCPDS, no. 22-044) indicate that α-MnO_2 nanosheets have been successfully prepared. As for the α-MnO_2–CNTs hybrids, the intensity of CNTs' diffraction peak decreased, indicating the modification of α-MnO_2 nanosheets with CNTs. Moreover, there are obvious and sharp characteristic peaks at 15.51°, 19.83°, 2.68° and 36.54°, which is diffraction peak related to α-MnO_2 nanosheets.[19,20] The XRD results indicate that α-MnO_2 nanosheets and α-MnO_2–CNTs hybrids flame retardants are synthesized successfully.

Fig. 2 is the SEM of α-MnO_2 nanosheets, α-MnO_2–CNTs hybrids and CNTs. As for α-MnO_2, it does not show layered morphology. As for α-MnO_2–CNTs hybrids, the α-MnO_2 and CNTs appear simultaneously in one system, and CNTs disperses on the surface of α-MnO_2. Moreover, it can be found that α-MnO_2 nanosheets are well growing adhered to CNTs. Combining with the XRD results, it shows that the α-MnO_2 and CNTs have been perfectly combined. The morphologies and structures of α-MnO_2 nanosheets, CNTs and α-MnO_2–CNTs hybrids are further investigated by TEM, as shown in Fig. 3. As for the TEM of CNTs, the diameter of CNTs is about 10 nm. As for the α-MnO_2 nanosheets, it can be found that the morphology is the layered structure. The structure of α-MnO_2–CNTs hybrids can be clearly found in Fig. 3, and CNTs nanostructures are well attached to α-MnO_2 nanosheet. The functional groups such as –COOH or –OH on the surface of CNTs supply the sites interacting with the Mn precursors during the preparing processes, resulting in good interaction and compatibility between CNTs and α-MnO_2. From the TEM of α-MnO_2–CNTs hybrids at high resolution, the CNTs are growing into the α-MnO_2 nanosheets. Thus, it can be concluded that the CNTs plays the base role on the growth of α-MnO_2 nanosheets, while α-MnO_2 nanosheets play the role in the uniform distribution of CNTs in the epoxy resins. As shown in Fig. 4, the TGA profiles of α-MnO_2 nanosheets and α-MnO_2–CNTs hybrids under nitrogen atmosphere are investigated. Both of α-MnO_2 nanosheets and α-MnO_2–CNTs hybrids have a mass loss at the temperature range of 200–400 °C. Compared with α-MnO_2 nanosheets, α-MnO_2–CNTs hybrids exhibit higher char residues at 400–700 °C, which is ascribed to the barrier effect of α-MnO_2 nanosheets and the char reinforcing effect of CNTs.[21]

3.2 Dispersion state of the flame retardants in EP composites

The dispersion as well as interfacial interaction between polymer matrix and the nano-fillers play important roles in the property reinforcement of composites materials. The SEM of the micro-morphology of brittle failure surfaces of the composites was investigated, as shown in Fig. 5. As for the

Fig. 2 SEM images of CNTs, α-MnO_2 and α-MnO_2–CNTs.

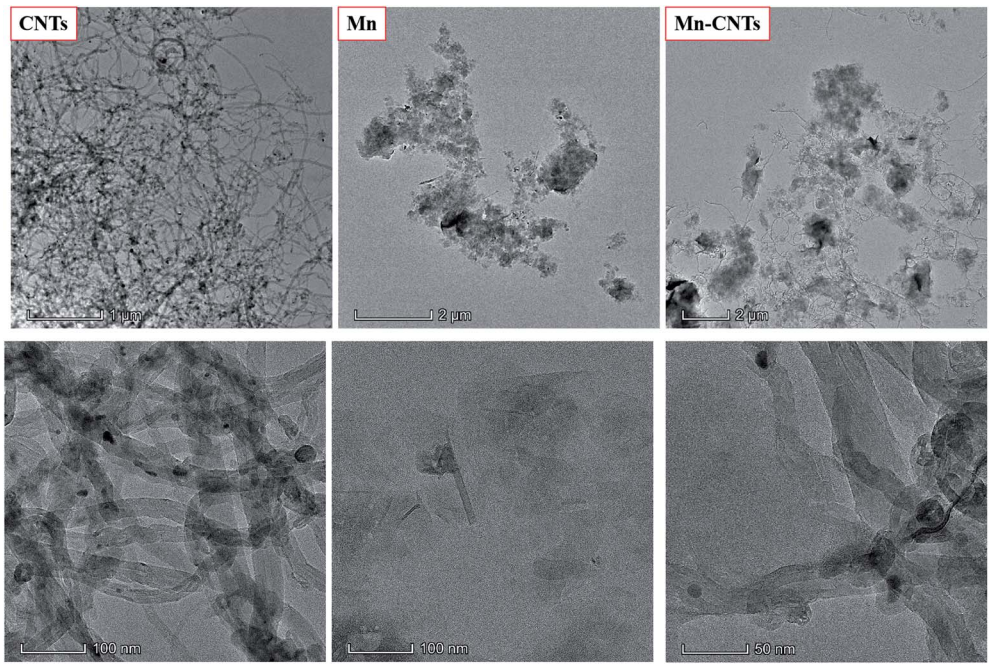

Fig. 3 TEM images of CNTs, α-MnO_2 and α-MnO_2–CNTs.

surface of EP, the surface is clean and smooth. As for the EP/Mn–CNTs composites, the fractured surface becomes rough and several particles can be observed at the surface or embed in the matrix. Moreover, it is obvious that there is no agglomeration phenomenon for the CNTs on the brittle failure surfaces of the composites. Generally, α-MnO_2–CNTs hybrids are well dispersed in the EP matrix, which is due to the fact that α-MnO_2 nanosheets and CNTs have synergistic dispersion effect.

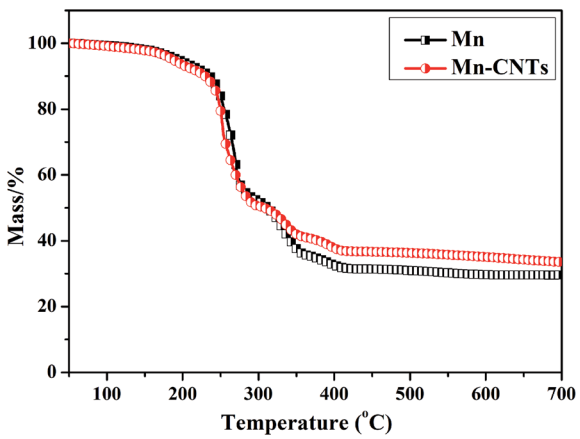

Fig. 4 TGA profiles for CNTs, α-MnO_2 and α-MnO_2–CNTs under nitrogen atmospheres.

3.3 The thermal stability of the composites

The thermal stability of EP and its composites was investigated by TGA, and the TGA and DTG curves of EP and its composites in nitrogen atmosphere are shown in Fig. 6 and the corresponding data are listed in Table 1. It can be found that EP have only one-stage degradation process, that's because the EP molecular chains decompose as the temperature increase. When CNTs, α-MnO_2 and α-MnO_2–CNTs hybrids were introduced into the EP matrix, the thermal stability of all composites is all improved obviously at high temperature, resulting in improved residues. For example, the residues for EP/CNTs composites at 700 °C are 16.5%. However, as those for the EP/α-MnO_2 composites, it increased to 17.5%. When the α-MnO_2–CNTs hybrids were added, the char residues at 700 °C increased

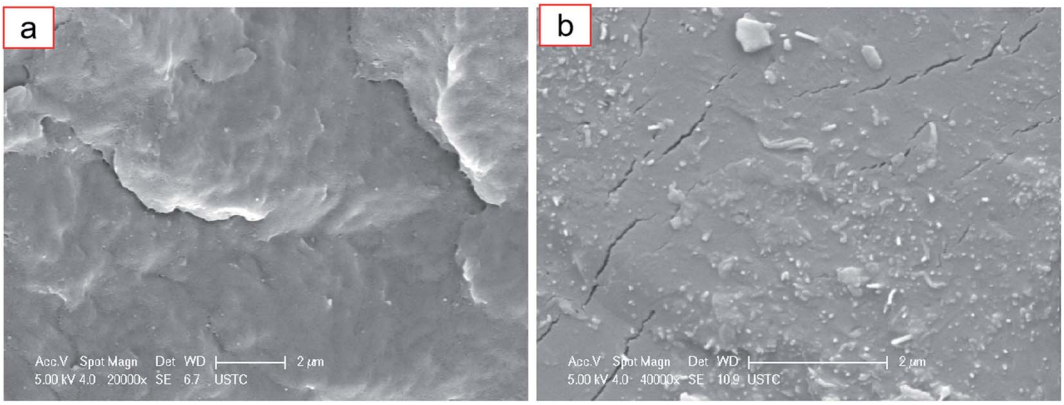

Fig. 5 SEM images of the fractured surface of EP (a), EP/Mn–CNTs composites (b).

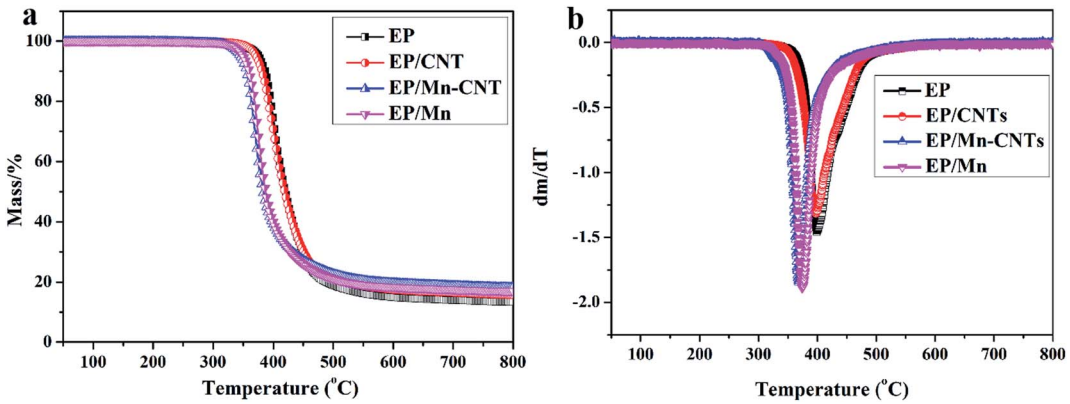

Fig. 6 TGA/DTG profiles for EP and its composites as function of temperature under nitrogen atmosphere.

to 18.9%, which is a great advance. In the previous work, it reported that the transition metal compound can be result in the early degradation of polymer materials.[23,24] In accordance with the previous reports, α-MnO_2–CNTs hybrids flame retardants can promote thermal degradation of EP composites, resulting in reduced thermal stability of EP resins. Moreover, the flame retardants in the composites can also decrease the T_{max} slightly. The EP/α-MnO_2–CNTs composites have the lowest $T_{-10\%}$ and T_{max} values. Generally, the catalyzing effect of transition-metal compound and the high thermal conductivity of carbon materials are responsible for the decreased thermal stability at low temperature. However, incorporation of either of CNTs and α-MnO_2 will result in higher char residues, indicating that α-MnO_2–CNTs hybrids flame retardants can inhibit the thermo-oxidative decomposition of epoxy resins and catalyze the formation of stable char layers at high temperature. Meanwhile,

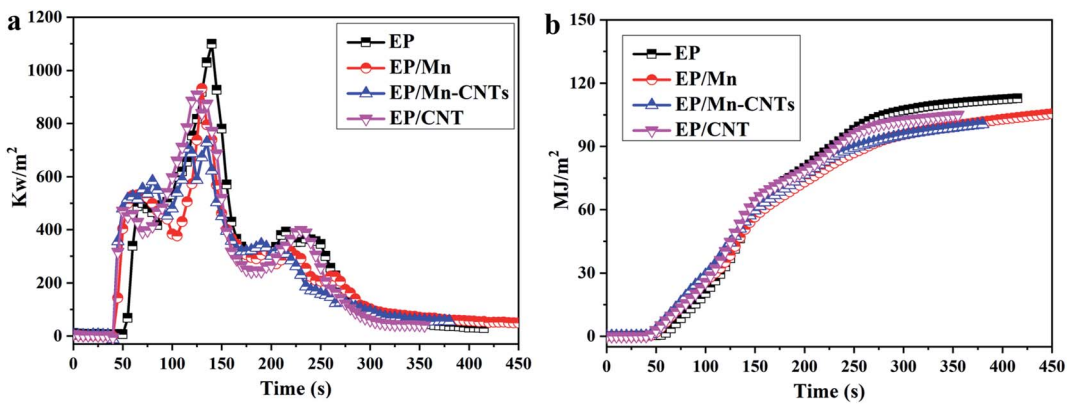

Fig. 7 Cone calorimeter test results: HRR and THR curves of EP and its composites.

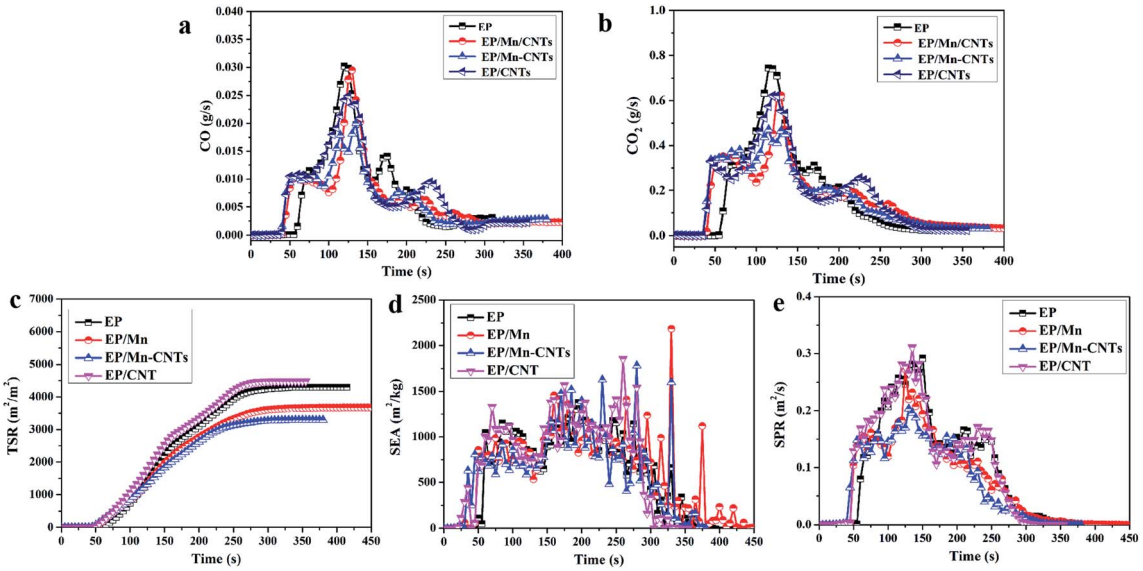

Fig. 8 Smoke release of EP and its composites during the cone test CO (a), CO_2 (b), TSR (c), SEA (d) and TSP (e).

the improved thermo-oxidative stability at high temperature of EP/α-MnO_2–CNTs composites is ascribed to the network structures of α-MnO_2 and CNTs, synergistic effect between α-MnO_2 and CNTs, the catalytic carbonization effect and physical barrier effect of α-MnO_2.

3.4 Fire hazard of EP and its composites

It is obvious that burning polymer could not only release huge amount of heat radiation but also lots of toxic smokes. The heat and smoke release are important factors for investigating the fire safety of polymer materials. The cone calorimeter is adopted to investigate the parameters such as peak heat release rate (pHRR), smoke production rate (SPR) and total smoke production (TSP), CO and CO_2 release to evaluate the fire safety properties of the EP.

The HRR and THR curves of pristine EP and its composites are shown in Fig. 7. The HRR and THR results indicate that the flame retardant properties of all the samples are improved. Compared with CNTs, α-MnO_2 behave more effectively in reducing the pHRR value of the composites. α-MnO_2 nanosheets perform better than CNTs in decreasing the flame retardancy of EP composites. Moreover, the pHRR value of EP/α-MnO_2–CNTs composites (728 kW m^{-2}) shows a 34.0% reduction compared with pure EP, which is the best optimal fire safety among all the samples. As for the THR values, it's found that the EP/α-MnO_2–CNTs composites have the lowest values, which is 10.7% reduction compared with pure EP. Generally, the composites with good α-MnO_2 nanosheet and CNTs dispersion are likely to form a continuous network structures, which is suggested by the SEM results.[8,25] The combination of CNTs and α-MnO_2 nanosheets can suppress the accumulation of both compounds in the composites and promote the uniform dispersion of the two nano-fillers in the EP matrix, resulting in improved the char reinforcing effect of CNT and catalytic carbonization effect of α-MnO_2.

Generally, the releasing of smoke and poisonous gases is harmful to human health, and smoke and poisonous gases often cause death in the fire accident. Therefore, reducing the releasing of toxic and harmful gas is not just scientific but social as well. The carbon monoxide (CO) releasing, carbon dioxide (CO_2) releasing, smoke production rate (SPR), specific extinction area (SEA) and total smoke production (TSP) curves of the composites are shown in Fig. 8. It can be found that the peak CO and CO_2 releasing values of all the composites are reduced. Among all the composites, EP/α-MnO_2–CNTs composites have the lowest peak CO and CO_2 releasing value, indicating the excellent toxic gas suppression properties of α-MnO_2–CNTs hybrids. Moreover, as for the smoke releasing, the effect of α-MnO_2–CNTs hybrids composites on the reducing the SPR and TSP is obvious among all the samples. Those indicate that α-MnO_2–CNTs hybrids flame retardants can catalyze the thermal oxidation of the composites and the carbon formation, which can be suggested by the TGA and Raman results.

3.5 Char residues of pure EP and its composites

It is well known that the char layers could play an important role in improving the flame retardant performance; thus it is very important to measure the char layers so as to investigate the flame retardant mechanism. As shown in Fig. 9, the char residues of all the composites after cone calorimeter tests are collected, which is used to further explore the flame retardant mechanism of the EP and its composites. It can be found that pure EP has few char residues after the cone test. As for the char residues of EP/α-MnO_2, EP/α-MnO_2–CNTs and EP/CNTs composites, it is obvious that the α-MnO_2 nanosheets in the composites can promote the formation of stable char layers, attributing to the catalysis effect and barrier effect of MnO_2 nanosheets. Moreover, the char layer of EP/α-MnO_2–CNTs composites are stable than those of EP/α-MnO_2 composites, which are due to the good dispersion of α-MnO_2 nanosheet and

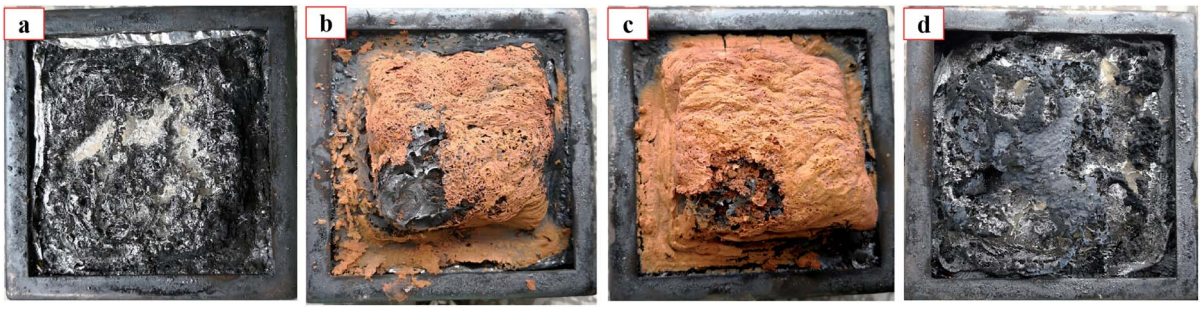

Fig. 9 Digital photo of the char residues of EP and its composites after the cone test: EP (a); EP/Mn composites (b); EP/Mn–CNTs composites (c); EP/CNTs (d).

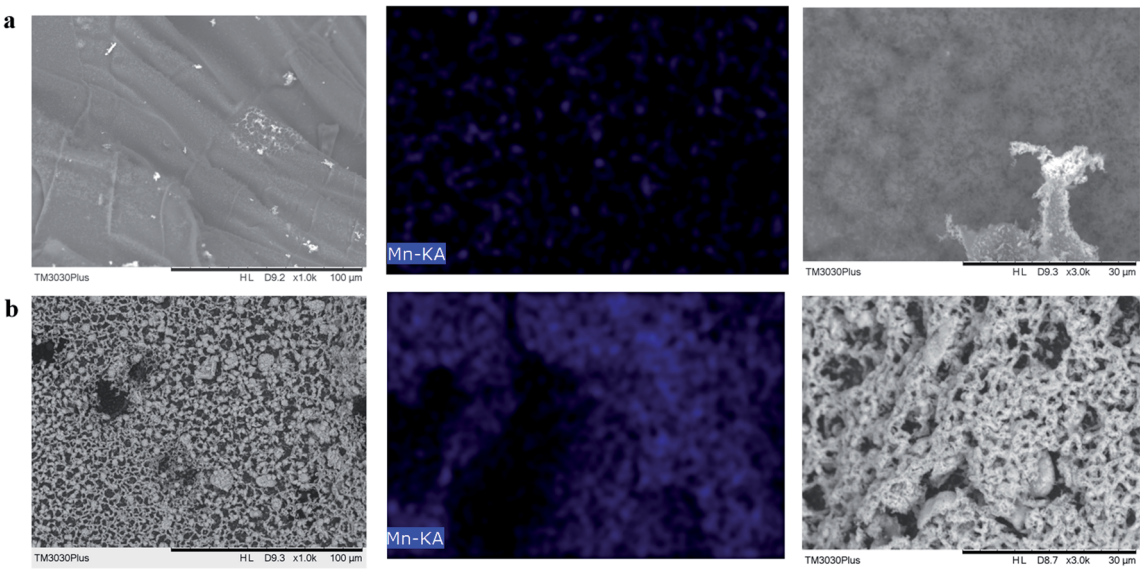

Fig. 10 The SEM and EDS of the char residues of EP/Mn (a) and EP/Mn–CNTs (b) after the cone test.

the network structure form by CNTs and α-MnO_2 nanosheets. Moreover, the surface of the char residues of EP/α-MnO_2 and EP/α-MnO_2–CNTs composites is covered with yellow substance. According to the previous report, the yellow substance is due to the indexed to the formation of Mn_3O_4.[22] Generally, Mn_3O_4 formed at high temperature can play the roles as the physical barrier to prevent the further permeation of heat, oxygen and combustible gases.

Fig. 10 is the SEM and EDS results of carbon residues for EP/α-MnO_2 and EP/α-MnO_2–CNTs composites. It can be found that the whole char layers of EP/α-MnO_2 composites are bumpy and extremely uneven, and the char layers exhibited a state of looseness. As for the char layers of EP/α-MnO_2–CNTs composites, it can be found that char layer has network structures, which is due to high thermostability of CNTs, and the Mn_3O_4 particles. The dispersion of Mn element on the char layers is determined by EDS, as shown in Fig. 11. Mn is derived from α-MnO_2–CNTs hybrids and it's found that the Mn elements disperse well compared with char layers of EP/α-MnO_2 composites. Thus, the EDS spectrum has further confirmed that the α-MnO_2 nanosheets disperse well in the composites due to the present of CNTs in the EP/α-MnO_2–CNTs composites. According to previous reports, CNTs can play its flame retardant roles through the formation of network-structured protective

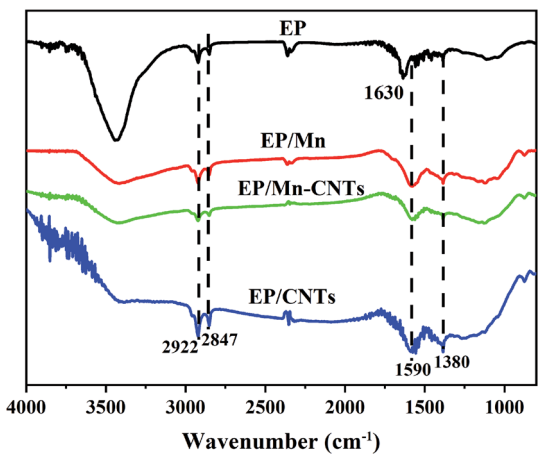

Fig. 11 FTIR of the char residues of EP and its composites after the cone test.

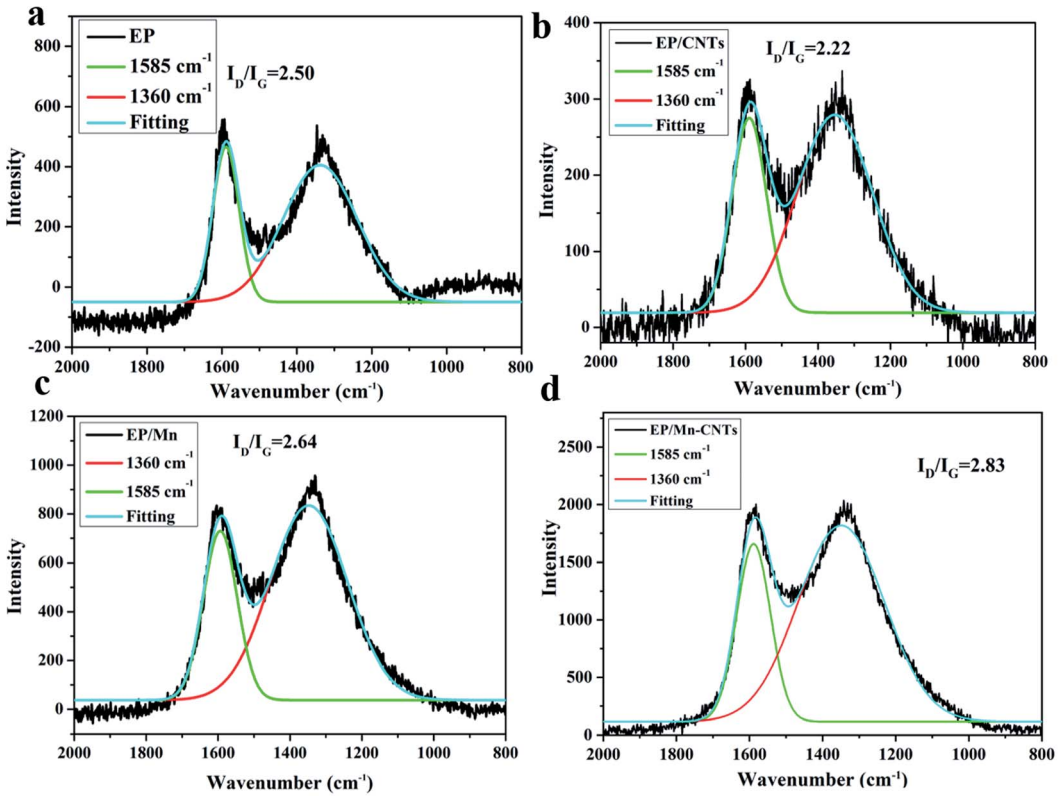

Fig. 12 Raman spectra of char residues of EP and its composites.

layer.[8] Generally, the α-MnO_2–CNTs hybrids flame retardants can catalyze the formation of stable char layers, and the char layer can effectively inhibit transferring of heat, oxygen and volatiles, resulting in improved fire safety.

The FTIR spectra of the char residues are collected in Fig. 11. The peaks at 2922 cm^{-1} and 2847 cm^{-1} correspond to the character peaks of alkane. Compared with pure EP, the peaks appearing at 1380 cm^{-1} and 1630 cm^{-1} are assigned to the vibrations of C=C in the aromatic compounds.[26,27] When CNTs and α-MnO_2 nanosheet were introduced into the EP matrix, the peak at 1630 cm^{-1} shifts to lower wavenumbers.[28,29] Raman spectroscopy is adopted to analyze the composition of carbon layer, as shown in Fig. 12. The Raman spectroscopy has two broad and strong peaks at about 1360 and 1585 cm^{-1}, the band at 1360 cm^{-1} (the D band) is due to the disordered graphite or glassy carbon, while the band at 1585 cm^{-1} (G band) is attributed to the stretching vibration mode with E_{2g} symmetry in the aromatic layers of crystalline graphite. Generally, the graphitization degree of the char layers is estimated by I_D/I_G (I_D and I_G are the integrated intensities of the D and G bands).[30,31] The higher graphitization degree of the char layers usually results in the lower ratio of I_D/I_G. As shown in Fig. 11, the sequence of I_D/I_G ratio is: EP/CNTs < EP < EP/Mn < EP/Mn–CNTs, those indicate that the char layers of EP/CNTs composites have the highest graphitization degree, which are due to the present of CNTs. The TGA results indicate that α-MnO_2 nanosheet or α-MnO_2–CNTs hybrids can catalyze the formation of stable char layers at high temperature. Thus, based on the Raman and TGA results, it can be concluded that the α-MnO_2 or α-MnO_2–CNTs can only create more glassy carbon during the thermal oxidative degradation process.

Generally, the mechanisms of α-MnO_2–CNTs hybrids on improving the fire safety of epoxy resins are as followings: the α-MnO_2 can not only decrease fuel gases diffusion during the thermal decomposition process of epoxy resins, but also catalyze the formation of stable char layers; the compact network structure formed by α-MnO_2 and CNTs can also suppress the releasing of fuel gases and toxic gases. Moreover, α-MnO_2–CNTs hybrids combine the advantages of the two nanofillers to form stable char layer structure with large area and heat-resistance, and those char layers can sever as an effective barrier to

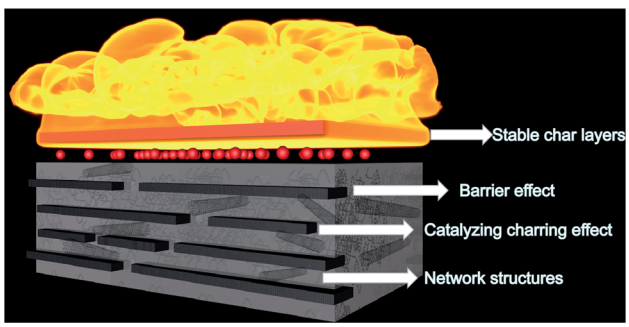

Scheme 2 The mechanism of α-MnO_2–CNTs hybrids in the flame retardancy of EP.

thermal transferring and releasing of organic volatiles, then the fire safety properties are improved. The mechanism is shown in Scheme 2.

4. Conclusion

To overcome the flammability and smoke toxicity releasing of epoxy resins, novel α-MnO_2–CNTs hybrids flame retardants were synthesized and epoxy composites at 2 wt% constant loading were prepared through thermal curing processes. The structures of α-MnO_2–CNTs hybrids flame retardants were confirmed by TEM and SEM. Moreover, the thermal stability of the composites was investigated by TGA and the flame retardant and smoke emission properties of epoxy composites were studied by cone calorimeter tests. The results showed that the fire safety properties of composites were improved significantly specially for EP/α-MnO_2–CNTs composites, and the toxic gases such as CO, CO_2 and TSR were reduced obviously. The improved fire safety properties were generally due to the network structures and the synergistic effect of α-MnO_2 and CNTs, the catalyzing charring effect, smoke suppression and physical barrier effect of α-MnO_2 nanosheets.

Conflicts of interest

There are no conflicts to declare.

Acknowledgements

This work was financially supported by National high-level talent special support plan project (Grant No. WRJH201801), Natural Science Foundation of China (Grant No. 21704111, 51674152), Fundamental Research Funds for China Academy of Safety Science and Technology (Grant No. 2020JBKY02), National key research and development program (Grant No. 2017YFC0805000).

References

1 Prateek, K. T. Vijay and K. G. Raju, Recent Progress on Ferroelectric Polymer-Based Nanocomposites for High Energy Density Capacitors: Synthesis, Dielectric Properties, and Future Aspects, *Chem. Rev.*, 2016, **7**, 4260–4317.

2 Y. B. Cui, S. I. Kundalwal and S. Kumar, Gas barrier performance of graphene/polymer nanocomposites, *Carbon*, 2016, **3**, 313–333.

3 C. Hyun and J. W. Jonggeon, Fabrication and characterization of multi-walled carbon nanotubes/polymer blendmembranes, *Membr. Sci.*, 2006, **11**, 406–415.

4 L. Kin, G. Chong and H. David, A critical review on nanotube and nanotube/nanoclay related polymer composite materials, *Composites, Part B*, 2006, **6**, 425–436.

5 M. Khan, F. Shahil and A. Alexander, Graphene–Multilayer Graphene Nanocomposites as Highly Efficient Thermal Interface Materials, *Nano Lett.*, 2012, **12**, 861–867.

6 Y. J. Li and S. Hiroshi, Conductive, PVDF/PA6/CNTs Nanocomposites Fabricated by Dual Formation of Cocontinuous and Nanodispersion Structures, *Macromolecules*, 2008, **4**, 5339–5344.

7 T. Kashiwahi, F. M. Du, J. F. Douglas and K. I. Winey, Nanoparticle networks reduce the flammability of polymer nanocomposites, *Nat. Mater.*, 2005, **4**, 928–933.

8 V. D. Punetha, R. Sravendra, J. Y. Hyen, C. Alok, J. T. McLeskey, M. R. Sekkarapatti, G. Nanda Sahooa and J. C. Whan, Functionalization of carbon nanomaterials for advanced polymer nanocomposites: a comparison study between CNT and graphene, *Prog. Polym. Sci.*, 2017, **67**, 1–47.

9 Ü. Deniz, D. Elif, B. Osman, Ç. Dilek and Ç. C. Fevzi, Composite Structures Understanding the polymer type and CNT orientation effect on the dynamic mechanical properties of high volume fraction CNT polymer nanocomposites, *Compos. Struct.*, 2016, **11**, 255–262.

10 J. N. Coleman, U. Khan, W. J. Blau and Y. K. Gun, Small but strong: a review of the mechanical properties of carbon nanotube–polymer composites, *Carbon*, 2006, **44**, 1624–1652.

11 W. Y. Xing, W. Yang, W. J. Yang, Q. H. Hu, J. G. Si, H. D. Lu, B. H. Yang, L. Song, Y. Hu and R. K. K. Yuen, Functionalized Carbon Nanotubes with Phosphorus- and Nitrogen Containing Agents: Effective Reinforcer for Thermal, Mechanical, and Flame-Retardant Properties of Polystyrene Nanocomposites, *ACS Appl. Mater. Interfaces*, 2016, **8**, 26266–26274.

12 J. T. Feng, J. H. Sui, W. Cai and Z. Y. Gao, Microstructure and Mechanical Properties of Carboxylated Carbon Nanotubes/Poly(L-lactic acid) Composite, *J. Compos. Mater.*, 2008, **42**, 1587–1595.

13 F. Yi, N. Anmin, M. Gregory and X. Rui, Asynchronous Crystal Cell Expansion during Lithiation of K+-Stabilized α-MnO_2, *Nano Lett.*, 2015, **15**, 2998–3007.

14 Z. P. Ma, G. J. Shao, Y. Q. Fan, G. L. Wang, J. J. Song and D. J. Shen, Construction of Hierarchical, α-MnO2 Nanowires@Ultrathin δ-MnO2 Nanosheets Core–Shell Nanostructure with Excellent Cycling Stability for High-Power Asymmetric Supercapacitor Electrodes, *ACS Appl. Mater. Interfaces*, 2016, **8**, 14.

15 S. V. Levchik, G. F. Levchik, G. Camino, L. Costa and A. I. Lesnikovich, Mechanism of Action of Phosphorus-basedFlameRetardantsin Nylon 6. III. Ammonium Polyphosphate/Manganese Dioxide, *Fire Mater.*, 1996, **7**, 4.

16 Y. Liu, Z. C. Zhao, C. J. Zhang, Y. Guo, P. Zhu and D. Y. Wang, Effect of manganese and cobalt ions on flame retardancy and thermal degradation of bio-based alginate films, *Mater. Sci.*, 2016, **1**, 1052–1060.

17 T. Dhanushk and T. P. Hapuarachchi, Multiwalled carbon nanotubes and sepiolite nanoclays as flame retardants for polylactide and its natural fibre reinforced composites, *Composites, Part A*, 2010, **8**, 954–963.

18 P. Kaushik, D. J. Kang, Z. X. Zhang and J. K. Kim, Synergistic Effects of Zirconia-Coated Carbon Nanotube on Crystalline Structure of Polyvinylidene Fluoride Nanocomposites: Electrical Properties and Flame-Retardant Behavior, *Langmuir*, 2010, **26**, 3609–3614.

19 W. Wang, Y. Pan, H. Pan, W. Yang, K. Liew and L. Song, Synthesis and characterization of MnO2 nanosheets based multilayer coating and applications as a flame retardant for flexible polyurethane foam, *Compos. Sci. Technol.*, 2016, **2**, 12–21.

20 C. C. Marius, J. H. Matthew, E. Manias and C. Giovanni, The influence of carbon nanotubes, organically modified montmorillonites and layered double hydroxides on the thermal degradation and fire retardancy of polyethylene, ethylene–vinyl acetate copolymer and polystyrene, *Polymer*, 2007, **10**, 6532–6545.

21 K. Kai, Y. Yoshida, H. Kageyama, G. Saito, T. Ishigaki, Y. Furukawa, *et al.*, Room, temperature synthesis of manganese oxide monosheets, *J. Am. Chem. Soc.*, 2008, **130**, 38–43.

22 W. Wang, Y. C. Kan, B. Yu, Y. Pan, K. M. Liew, L. Song and Y. Hu, Synthesis of MnO_2 nanoparticles with different morphologies and application for improving the fifire safety of epoxy, *Composites, Part A*, 2017, **95**, 173–182.

23 X. Feng, W. Xing, L. Song and Y. Hu, In situ synthesis of a MoS_2/CoOOH hybrid by a facile wet chemical method and the catalytic oxidation of CO in epoxy resin during decomposition, *J. Mater. Chem. A*, 2014, **2**, 299–308.

24 A. M. Asiri, M. A. Hussein, B. M. Abu-Zied and A. E. A. Hermas, Effect of NiLaxFe2 xO4 nanoparticles on the thermal and coating properties of epoxy resin composites, *Composites, Part B*, 2013, **1**, 1–8.

25 X. D. Qian, L. Song, B. Yu, B. B. Wang, B. H. Yuan, Y. Q. Shi, Y. Hu and K. K. Richard, Novel organic–inorganic flame retardants containing exfoliated graphene: preparation and their performance on the flame retardancy of epoxy resins, *J. Mater. Chem. A*, 2013, **1**, 6822–6830.

26 K. L. Gong, K. Q. Zhou and B. Yu, Superior thermal and fire safety performances of epoxy-based composites with phosphorus-doped cerium oxide nanosheets, *Appl. Surf. Sci.*, 2020, **504**, 144314.

27 K. Q. Zhou, G. Tang, R. Gao and S. D. Jiang, In situ growth of 0D silica nanospheres on 2D molybdenum disulfide nanosheets: towards reducing fire hazards of epoxy resin, *J. Hazard. Mater.*, 2018, **344**, 1078–1089.

28 X. D. Qian, H. F. Pan, W. Y. Xing, L. Song, R. K. K. Yuen and Y. Hu, Thermal Properties of Novel 9,10-Dihydro-9-oxa-10-phosphaphenanthrene 10-Oxide-based Organic/Inorganic Hybrid Materials Prepared by Sol-Gel and UV-Curing Processes, *Ind. Eng. Chem. Res.*, 2012, **51**, 85–94.

29 K. Wu, L. Song and Y. Hu, Synthesis and characterization of a functional polyhedral oligomeric silsesquioxane and its flflame retardancy in epoxy resin, *Prog. Org. Coat.*, 2009, **65**, 490–497.

30 A. Sadezky, H. Muckenhuber, H. Grothe, R. Niessner and U. Poschl, Raman microspectroscopy of soot and related carbonaceous materials: Spectral analysis and structural information, *Carbon*, 2005, **43**, 1731–1742.

31 B. J. Landi, H. J. Ruf, C. M. Evans, C. D. Cress and R. P. Raffaelle, Purity Assessment of Single-Wall Carbon Nanotubes, Using Optical Absorption Spectroscopy, *J. Phys. Chem. B*, 2005, **109**, 9952–9965.